

# Experimental Optics

**Contact person:**

Roland Ackermann

Friedrich-Schiller-Universität Jena

Abbe School of Photonics

Max-Wien-Platz 1

07743 Jena, Germany

Phone: +49 3641 9-47821, e-mail : [Roland.Ackermann@uni-jena.de](mailto:Roland.Ackermann@uni-jena.de)

**Last edition:** Roland Ackermann, February 2015

**Lab Title:**

<b>Group number</b>	G 14
<b>Student name(s)</b>	Ke Li, Jerome Jahn
<b>Name of TA</b>	Markus Blothe
<b>Date of Lab</b>	Feb 28, 2019
<b>Date of Final Report return</b>	March 4, 2019

# Neodymium YAG Laser Report

Ke Li, Jerome Jahn

March 2019

## Contents

<b>1</b>	<b>Introduction</b>	<b>3</b>
<b>2</b>	<b>Theory</b>	<b>3</b>
2.1	Nd:YAG Laser System . . . . .	3
2.2	Q-Switching . . . . .	4
2.2.1	Active Q-Switching . . . . .	4
2.2.2	Passive Q-Switching . . . . .	5
<b>3</b>	<b>Experimental Procedures</b>	<b>6</b>
3.1	Experiment Setup . . . . .	6
3.2	Laser Diode as Pump Laser . . . . .	6
3.2.1	Characterizing the pump laser diode . . . . .	6
3.2.2	Focusing . . . . .	7
3.2.3	Nd:YAG rod characteristics . . . . .	7
3.2.4	Nd:YAG laser resonator . . . . .	7
3.3	Q-Switching . . . . .	7
3.3.1	Active Q-Switching . . . . .	7
3.3.2	Passive Q-Switching . . . . .	8
3.3.3	Frequency doubling of the laser wavelength . . . . .	9
<b>4</b>	<b>Results</b>	<b>9</b>
4.1	Characterize the Pump Laser . . . . .	9
4.1.1	Minimum Injection Current . . . . .	9
4.1.2	Pump Laser Output Power as Function of Temperature .	12
4.2	Focusing the Beam . . . . .	13
4.3	Nd:YAG Rod Characteristics . . . . .	13
4.3.1	Absorption Spectrum . . . . .	13
4.4	Nd:YAG Laser Resonator . . . . .	17
4.4.1	Pump Current and Laser Output Power Result . . . . .	17
4.4.2	Pump Laser Modulation and Modes of Output Lasers .	19
4.5	Active Q Switching and Measurements of Critical Parameters .	19
4.5.1	Output pulse energy as a function of the Q-switch delay .	19
4.5.2	Output Pulse Energy vs. Pump Rate . . . . .	21

4.6	Investigation of Passive Q-Switching . . . . .	23
4.6.1	Frequency vs. Q-Switching Peaks . . . . .	23
4.6.2	Pump Laser Power vs. Passive Absorber Peaks . . . . .	24
4.6.3	Absorber-YAG Rod Distance and Characters of Peaks . .	25
4.6.4	Frequency Doubling of the Laser Wavelength . . . . .	25
<b>5</b>	<b>Discussion</b>	<b>27</b>
5.1	Diode Laser Characterization . . . . .	27
5.1.1	Minimum Injection Current . . . . .	27
5.1.2	Pump Laser Output Power as a Function of Temperature	27
5.2	Nd: YAG Rod Characterization . . . . .	27
5.2.1	Absorption Spectrum . . . . .	27
5.3	Nd:YAG Laser Resonator . . . . .	27
5.4	Active Q-Switching . . . . .	28
5.5	Passive Q-Switching . . . . .	28
<b>6</b>	<b>Conclusion</b>	<b>28</b>
6.1	Second Harmonic Generation . . . . .	29
<b>7</b>	<b>References</b>	<b>29</b>

# 1 Introduction

The goal of this set of experiments was to investigate various laser configurations using a neodymium-doped yttrium aluminum garnet (Nd:YAG) crystal as the lasing medium. In particular, a continuous wave laser outputting 1064 nm, an actively Q-switched pulsed laser, a passively Q-switched pulsed laser and a continuous wave laser outputting 532 nm were constructed.

The Nd:YAG laser is one of the most popular solid-state lasers used in research and technology. The lasing medium was first used at Bell laboratories in the 1960's and has since been used in applications ranging from hair removal and laser hypolysis to military applications including target designation and ranging as well as finding use in blinding laser weapons.

Using Q-switching, laser pulses on the time span of nanoseconds can be generated carrying powers in the range of MegaWatts. While the fastest and strongest lasers nowadays emit attosecond pulses with powers up to multiple PetaWatts, Q-switched lasers remain widespread. Increased understanding of the properties of this method for generating pulses as well as of the Nd:YAG laser was the overall aim of this set of experiments.

# 2 Theory

## 2.1 Nd:YAG Laser System

The Nd:YAG lasing medium is a doped crystal. The Neodymium ions replace the yttrium ions in the crystal lattice. The energy transitions of these neodymium ions are used in the laser process.

Lasers require an energy pump process, a lasing medium, and an optical resonator cavity. The pump process elevates electrons in lower energy levels in the lasing medium into energy levels typically higher than the energy level with energy separation from the ground state equal to the wanted energy of the emitted photon.

These recently elevated electrons then spontaneously decay into the lasing energy level very quickly, where the rate of decay due to spontaneous emission is usually much slower. If the pump rate, or electrons pumped into higher levels per second, is faster than the rate of decay due to spontaneous emission, the lasing energy level can be filled up quicker than it is depleted by spontaneous emission. This allows for the generation of a population inversion, or an overload of electrons in higher energy levels that are ready to be knocked down into lower energy levels. This population inversion can be turned into an avalanche of electrons jumping down to the same lower energy level, resulting in an emitted frequency that has much greater intensities than all other frequencies being generated from the continuously occurring spontaneous emission.

It is important to note that this build-up cannot be continued indefinitely. In fact, the rate of electrons jumping from a particular energy level  $\frac{dN}{dt}$  is inversely proportional to the decay time  $\tau$  and directly proportional to the number of

electrons in that energy level  $N$ , as shown in Eq. (1)

$$\frac{dN}{dt} = \frac{N}{\tau}. \quad (1)$$

The pump rate needs to be higher than the above product. The pump rate in a laser is controlled by the energy pump. This can be a diode laser. The pump rate is then proportional to the number of incident photons with the required energy levels to excited electrons into energy levels with (ideally much) faster spontaneous emission decay. Although many energy levels in the lasing medium may fulfill this condition, usually the laser is designed with knowledge of the specific energy level to be used. This results in most laser involving at most 4 energy levels, as they are mostly three or four-level systems. With only one energy level to be pumped to, the pump rate can be calculated from Eq. (2) below

$$R_p = P_{abs}/E_{photon}. \quad (2)$$

where  $P_{abs}$  is the absorbed power from the narrow bandwidth pump source and  $E_{photon}$  the energy separation between the ground level and the excited level from which electrons will decay to the lasing level.

The decay time due to spontaneous emission is defined as the time that it takes 63% of the electrons in a level to decay. This time is chosen as spontaneous decay is an exponential decay process, as indicated by Eq.

The laser cross section describes the probability of the incoming photon interacting with the neodymium ions to incur absorption or stimulated emission.

## 2.2 Q-Switching

The Q-factor of a resonator is a measure of the loss of the cavity, or a measure of the energy damping of the resonator as light reflects back and forth. If the Q-factor is high, then the losses are low, and the dissipated energy is a small portion of the electromagnetic energy carried by the resonating light. If the Q-factor is low, then the dissipated energy is a larger portion of the electromagnetic energy carried by the resonating light.

Q-switching involves changing the Q-factor of the cavity from low to high in order to achieve the emission of a pulse of laser light. This corresponds to transforming the laser cavity as one with high losses to a cavity with low losses. The quicker and the more dramatic the Q-switching, the more energetic the pulse.

### 2.2.1 Active Q-Switching

Active Q-switching usually involves going from an open cavity to a closed cavity in order to form a pulse of stimulation-emitted light.

### 2.2.2 Passive Q-Switching

The passive Q Switching is a Q Switching process utilizing the non-linear effect of a saturable absorber to create a population inversion process. As Figure 1 shows(1), a low intensity of light excites the ground state electrons to a higher energy level, causing stimulated emission. When the intensity of light becomes higher, none of the electrons are in the ground state level, which means that the absorber become a good transmittance of light. (1)

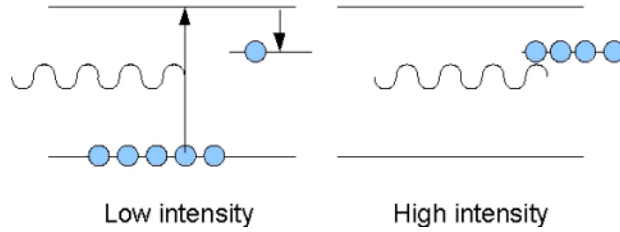


Figure 1: Saturable Absorber

Based on the mechanism shown in Figure 1, we could build up a passive Q-Switching process with the saturable absorber. As shown in Figure 2 below, at the first beginning, the energy flux of photon is low, thus resulting in a cavity with strong losses. The increase of the amount of the injection photons will cause a saturation inside the absorber, resulting in the decrease in the loss of the cavity. When the population inversion goes above the threshold, short laser pulsed will be generated, bringing up the losses of the cavity again, resulting in a new cycle of population inversion and the saturation of the absorber. (1)

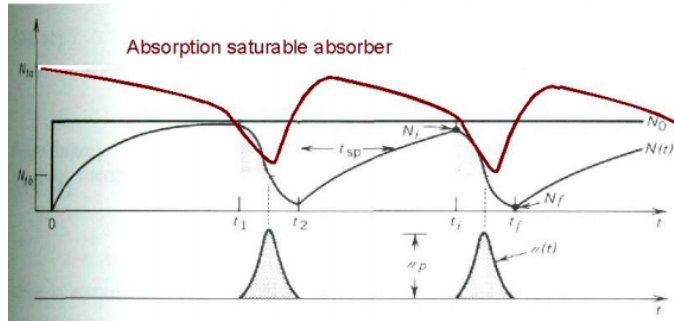


Figure 2: Passive Q Switching by Saturable Absorber

### 3 Experimental Procedures

#### 3.1 Experiment Setup

In this experiment, we used an experiment setup as shown in Figure 3 (?):

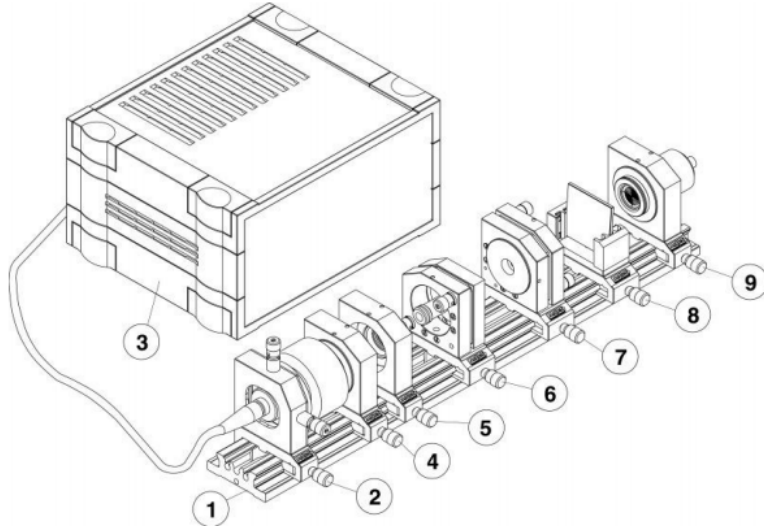


Figure 3: Experimental Setup

1 is a 500mm flat optical rail with scale. 2 is a laser diode with a power of 450 mW in X-Y adjustment holder on carrier. 3 is the control electronics LDS 1200 which is used to modulate and supply power to the pump laser diode shown in 2. 4 is a beam shaping optics in holder on carrier. 5 is the beam focusing in holder on carrier with a focal length of 60 mm. 6 is the Nd:YAG crystal and laser mirror. 7 is a concave laser mirror. 8 is a filter holder, with filter supplies of RG 1000, a long-pass filter, NG9 a density filter, and BG39. 9 is a photo detector(a photodiode) connected to an oscilloscope where we view the signal output.

#### 3.2 Laser Diode as Pump Laser

##### 3.2.1 Characterizing the pump laser diode

The laser diode was turned on and aimed at the photodiode connected to an oscilloscope. First, the dependence of the pump output power, encoded in the voltage on the oscilloscope, as a function of the injection current was found. The minimum injection current was determined from this data.

Next, the output power's dependence on the temperature of the laser diode was found. At temperatures higher than 30 degrees Celsius, the laser diode

was not given much time to adjust in a new thermal equilibrium, due to this temperature being outside of the range of the normal operating temperature, and the lifetime of the laser diode being reduced.

### 3.2.2 Focusing

The position of the beam focus was determined after having inserted a lens after the pump laser beam and using white cardboard to find where the spot size of the beam was at a minimum.

### 3.2.3 Nd:YAG rod characteristics

The Nd:YAG rod was inserted on a mount into the setup after the lens. It was positioned such that the beam was focused onto the back edge of the Nd:YAG rod. In this way, the properties of the Nd:YAG rod were investigated through the use of the photodiode.

The transmitted voltage as a function of the temperature of the rod was found by scanning through a range of wavelengths on the pump laser by changing the temperature from 15 to 35 degrees Celsius in 1 Celsius steps.

Then, the decay time for spontaneous emission was found

### 3.2.4 Nd:YAG laser resonator

In this part of the experiment, we studied the properties of the Nd:YAG laser resonator. In this experiment, we placed a reflective mirror behind the Nd:YAG rod to form a resonating cavity, and set the temperature of the pump laser diode to 28 degree as found from the previous experiments so that the absorption of the pump in the Nd:YAG laser is maximum. We used a long-pass filter RG 1000 to filter wavelength that is shorter than 850 nm, thus ensuring only wave with wavelength of 1064 nm is incident on the photo-diode. When the photo-diode was saturated when the injection current of the pump was raised to a higher value, we used the density filter NG 9. We adjusted the reflective mirror tilt so that only single transverse mode was observed in the oscilloscope, helping us getting maximum output from the photo-diode.

## 3.3 Q-Switching

### 3.3.1 Active Q-Switching

In this part of the experiment, we investigated Active Q- Switching method using Pockels cell unit. We placed a Pockel cell inside the Nd:YAG laser cavity . We set the modulation of the pump laser to rectangle mode with maximum injection current and aligned the cavity so that the output voltage shown oscilloscope is at it's maximum value. Before turning on the high voltage power supply to the Pockel cell, we set the trigger delay to about  $200\mu s$  and bring the voltage to 0 V. After turning on the high voltage supply to the Pocket cell, we and slowly

turned up the voltage of the supply until we observed a sharp spike as shown in Figure 4

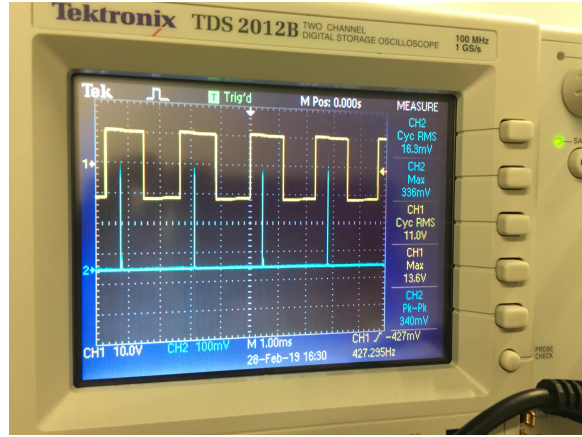


Figure 4: Intense Voltage Spike

### 3.3.2 Passive Q-Switching

In this part of the experiment, we investigated different characteristics of a passive Q-Switching. Before inserting a saturable absorber inside the laser cavity, we first optimize the emission of the YAG laser cavity by moving the YAG crystal and optimize the title of both mirrors of the cavity. In this experiment, we set the pump laser injection current to its' maximum value, and use a modulation of a square wave function. After the system is properly aligned, and we saw multiple Q-Switching peaks on the oscilloscope for each square wave pulse, we then investigated the characteristics of the passive Q-switching system interns of frequency of the laser modulation, the pump laser power , and the position of the saturable absorber inside the cavity.

Figure 5 below shows the correct output on the oscillator for a passive Q-Switching.

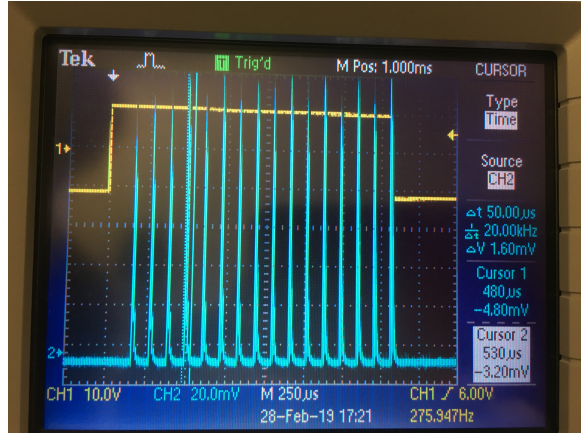


Figure 5: Passive Q Switching Output on Oscilloscope

### 3.3.3 Frequency doubling of the laser wavelength

In this part of the experiment, we investigated the relation between pump current and SHG laser output power. We placed a KTP crystal inside the laser cavity to generate double frequency of the Nd:YAG laser. The filter used in this experiment was BG39, which blocks all the IR radiation and the green radiation passes with an attenuation of about 40%. ( ). Before beginning measurement, we set the pump current to its maximum (560 mA), and used 28 ° as it is found as the best absorption in the Nd:YAG rod.

## 4 Results

### 4.1 Characterize the Pump Laser

#### 4.1.1 Minimum Injection Current

The behavior of the laser diode output power as a function of the injection current is given in Table 1. The temperature of the laser diode during these measurements was 25 °C. Starting with injection currents of 200 mA, the neutral density filter NG9 was inserted.

Injection Current (mA)	Max Voltage Output (mV)
0	Noise
25	Noise
50	6.08 ± 0.4
75	10.5 ± 2
100	21.5 ± 1
125	39.2 ± 2
150	83.2 ± 4
175	432 ± 20
200	53.6 ± 2
225	102 ± 4
250	144 ± 10
275	188 ± 10
300	228 ± 10
325	264 ± 10
350	300 ± 20
375	340 ± 20
400	376 ± 20
425	408 ± 20
450	440 ± 20
475	476 ± 20
500	510 ± 20
525	552 ± 20
550	574 ± 20
560	586 ± 20

Table 1: Photodiode Voltage as function of Diode Laser Injection Current

The values of  $1.8 \pm 3$  mV were chosen for the lower currents where only noise was shown. In order to compare the measurements with the neutral density filter inserted with the ones without, a scaling factor needed to be found. The scaling factor  $\beta$  is of the form in Eq. (3)

$$\beta = V_0/V_1, \quad (3)$$

where  $V_0$  is the voltage on the photodiode without the neutral density filter and  $V_1$  is the voltage on the photodiode with the neutral density filter inserted. The group measured at 175 ° C the photodiode voltage with the neutral density filter in place and without. The voltage without the filter is written in the table above. The voltage with the filter in place was  $6.54 \pm 2.5$  mV. The scaling factor is then found to be  $\beta = 66.055$ .

Table 2 shows the adjusted voltage values, with each voltage value being what it would be without the filter in place. The values with the filter as well as their uncertainties were multiplied by the scaling factor.

Injection Current (mA)	Photodiode Voltage (V)
0	Noise
25	Noise
50	.0061 ± 0.0004
75	.0105 ± .002
100	.0215 ± .001
125	.0392 ± .002
150	.0832 ± .004
175	.432 ± .02
200	3.5405 ± .132
225	6.7376 ± .264
250	9.5119 ± .661
275	12.418 ± .661
300	15.061 ± .661
325	17.439 ± .661
350	19.817 ± 1.321
375	22.459 ± 1.321
400	24.837 ± 1.321
425	26.95 ± 1.321
450	29.064 ± 1.321
475	31.442 ± 1.321
500	33.688 ± 1.321
525	36.462 ± 1.321
550	37.916 ± 1.321
560	38.708 ± 1.321

Table 2: Photodiode Voltage as function of Diode Laser Injection Current corrected for neutral density filter NG9

In order to graph the output power of the laser as a function of the injection current, the photocurrent is needed. As the photocurrent generated in the photodiode is not known, the group used the fact that since the oscilloscope updates roughly every 20 ns, and the period of optical light is on the order of  $10^{-14}$  s, the voltage shown on the oscilloscope is proportional to the power incident on the oscilloscope. Without actually performing this conversion, Figure 6 shows the lineshape of the output power graph.

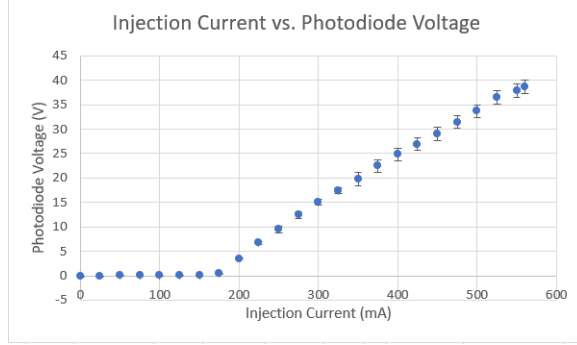


Figure 6: Photodiode Measurement Values for Diode Laser Injection Current with Laser Temperature 25 Degrees Celsius

A linear fit was performed on the data from 175 mA onwards in order to estimate the minimum injection current. The minimum value would be the x-intercept of the linear fit line. This fit is shown in Figure 7.

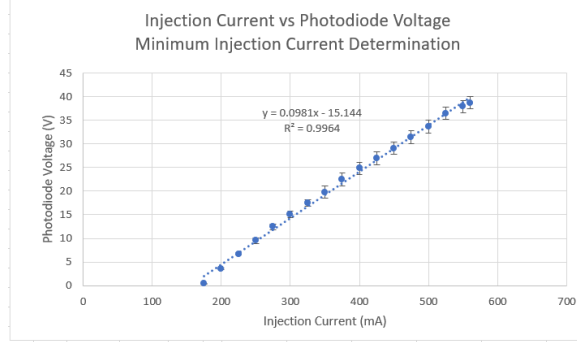


Figure 7: Determination of Minimum Injection Current

The equation of the trendline is shown in the above figure. The x-intercept of this line, signifying the minimum injection current to have lasing, or the lasing threshold, is at 154.4 mA. The slope efficiency is simply the slope shown in the above figure, at a value of .0981 V/mA.

#### 4.1.2 Pump Laser Output Power as Function of Temperature

The results of the photodiode voltage as a function of the diode laser temperature are shown in Table 3. The injection current was set to its maximum value of 560 mA during these measurements.

Temperature (°C)	Max Voltage Output (mV)
20	600 ± 40
23	592 ± 40
26	584 ± 40
29	576 ± 20
32	564 ± 20
35	560 ± 20

Table 3: Caption

The data is represented graphically in Figure 8.

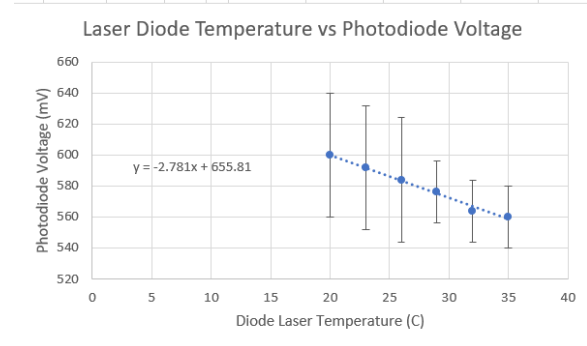


Figure 8: Photodiode Voltage as a function of the Diode Laser Temperature

The voltage on the photodiode being proportional to the power of the diode laser's output, it can be seen that there is an approximately linear relationship. As temperature of the diode increases, the output power decreases. The uncertainty in the measurements was determined to be tied to the scale of the oscilloscope reading used.

## 4.2 Focusing the Beam

The beam focus was found to be at position  $7.0 \pm .5$  centimeters in front of the lens.

## 4.3 Nd:YAG Rod Characteristics

### 4.3.1 Absorption Spectrum

The photodiode voltage as a function of the pump laser temperature is shown in Table 5. For temperatures 15-18 °C, the neutral density filter NG9 was used to avoid saturating the photodiodes.

Temperature (°C)	Max Voltage Output (mV)
15	17 ± 2
16	14.8 ± 2
17	13.6 ± 2
18	11.6 ± 2
19	640 ± 40
20	560 ± 40
21	544 ± 40
22	576 ± 40
23	576 ± 20
24	520 ± 20
25	496 ± 20
26	392 ± 40
27	352 ± 40
28	228 ± 40
29	232 ± 20
30	285 ± 20
31	520 ± 40
32	800 ± 100
33	1030 ± 40
34	1360 ± 200
35	1220 ± 100

Table 4: Pump Temperature vs Laser Voltage Output

A scaling factor was used to account for the implementation of a neutral density filter of type NG9 to avoid saturating the photodiode. The scaling factor was calculated from the value of the voltage at 19 degrees Celsius, measured at  $9.69 \pm 2$  mV with the density filter. The scaling factor  $\beta$  was then as in Eq.

$$\beta = \frac{V_{without}}{V_{with}} = 66 \quad (4)$$

The corrected data is then in Table

Temperature (°C)	Max Voltage Output (mV)
15	1120 ± 132
16	976.8 ± 132
17	897.6 ± 132
18	765.6 ± 132
19	640 ± 40
20	560 ± 40
21	544 ± 40
22	576 ± 40
23	576 ± 20
24	520 ± 20
25	496 ± 20
26	392 ± 40
27	352 ± 40
28	228 ± 40
29	232 ± 20
30	285 ± 20
31	520 ± 40
32	800 ± 100
33	1030 ± 40
34	1360 ± 200
35	1220 ± 100

Table 5: Pump Temperature vs Laser Voltage Output

The uncertainty of the first four values is so high as the uncertainty measurement was tied to the scale of the oscilloscope used. For larger measurements, the relative uncertainty is less, while for smaller measurements with the oscilloscope, the relative uncertainty is higher.

This data is plotted on a Cartesian graph in Figure 9.

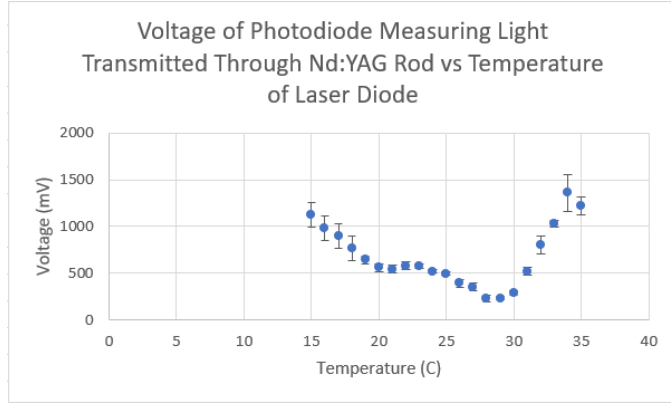


Figure 9: Voltage on Photodiode from Light Coming From Laser Diode with Variable Temperature Passing Through the Nd:YAG Crystal

The minimum in a transmission graph corresponds to the maximum in an absorption graph. It can be seen that, as with increasing temperature the photodiode wavelength also increases, the optimal emission wavelength when the diode laser is being operated at the full injection current corresponds to the wavelength at the minimum photodiode voltage, namely the wavelength being emitted when the laser diode is being run with 560 mA at 28 degrees Celsius.

This wavelength can be calculated with Eq. (5)

$$\lambda_0 = .27778(T) + 800.24, \quad (5)$$

as is done in Eq. (6)

$$\lambda_0 = .27778(28) + 800.24 = 808, \quad (6)$$

resulting in an experimentally determined optimal pumping wavelength of 808 nanometers. This wavelength is absorbed most. This corresponds to an energy as solved in Eq. (7)

$$E = \frac{hc}{\lambda} = \frac{(6.63e - 34)(3e8)}{808e - 9} = 2.5e - 19 Joules. \quad (7)$$

The pump rate in electrons per second is can be estimated by dividing the absorbed power of the material by the energy of the central photon in the emitted lineshape (calculated above) incident on the material. It needs to be the absorbed power as opposed to the incident power as the absorbed power is the absorbed energy per unit of time. As only energy packets corresponding to the separation between electronic energy levels are absorbed in this case, each absorbed photon corresponds to a "pumped up" electron. The pump rate equation is shown in Eq. (2).

The calculation of the power absorbed by the material begins with determining the incident power on the lasing material, then finding the fraction that was absorbed by considering the fraction of the voltage that was transmitted.

From Table 5, with the voltage on the oscilloscope being proportional to the power hitting the photodiode, it can be stated that at 28 degrees Celsius, the diode laser is outputting the power fraction stated in Eq. (8)

$$\frac{P_{28}}{P_{25}} = \frac{V_{28}}{V_{25}} = \frac{(655.81 - 2.781(28))}{(655.81 - 2.781(25))} = .985. \quad (8)$$

As oscilloscope voltage is proportional to power, the voltage ratio is the same. The output power of the laser rod can be attained by multiplying the incident power by the fraction in Eq. (9)

$$P_{out} = P_{inc} \frac{V_{withlaserrod}}{V_{withoutlaserrod}}, \quad (9)$$

The incident power on the rod is the output power of the diode laser operating with 560 mA at a temperature of 28 degrees Celsius. This output power is calculated in Eq. (10)

$$P_{inc} = .45W * .985 = .44W. \quad (10)$$

The absorbed power is then calculated in Eq. (11)

$$P_{abs} = P_{inc}(1 - \frac{V_{withlaserrod}}{V_{withoutlaserrod}}) = .44(1 - (228/578)) = .27W. \quad (11)$$

The pump rate is then estimated to be as in Eq. (12)

$$R_p = \frac{.27W}{2.5e - 19J} = 1.1e181/s, \quad (12)$$

## 4.4 Nd:YAG Laser Resonator

### 4.4.1 Pump Current and Laser Output Power Result

To measure evaluate the relation between pump current and the output power of the cavity, We adjusted the injection current from 0 to 560 mA, with a step of 50 mA, and measured the corresponding maximum output voltage on the photo-diode. The experiment data is shown in Table. After the current was raised above 400 degree, the photo-diode was saturated, we placed a density filter, and obtain the voltage value by multiplying the scaling factor introduced by the density filter. In this case, the scaling factor is: 98.82.

Injection Current (mA)	Max Voltage Output (V)
0	noise
50	noise
100	noise
150	noise
200	noise
250	noise
300	$0.468 \pm 0.02$
350	$1.1 \pm 0.1$
400	$1.68 \pm 0.1$
450	$2.36 \pm 0.2$
500	$2.7 \pm 0.2$
550	$3.2 \pm 0.2$
560	$3.36 \pm 0.2$

Table 6: Pump Current vs. Laser Output Power Experiment Data

Neglecting the data points where only noises were recorded, we plot the injection current and the maximum voltage on the photo-diode and implemented a linear fit. The result is shown in Figure 10

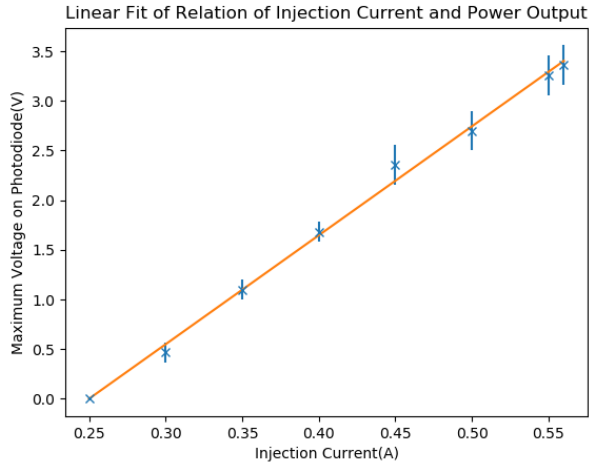


Figure 10: Linear Fit Result of Nd:YAG Cavity Output Power and Injection Current

As we can observe from Figure 10, the output voltage and injection current follows a linear relationship. The slope of the curve is  $10.97 \pm 0.8797$ , the intercept o the curve is  $-2.74 \pm 0.38$ , the p-value of the linear fit is  $1.398 \times 10^{-8}$ . The small p-value indicates that we can safely reject the null hypothesis that the two quantity we investigated are not linearly related. From this linear relation

we obtained, we can calculate the threshold of injection current:

$$x_{threshold} = -\frac{intercept}{slope} = 0.246A \quad (13)$$

The uncertainty of this calculation can be found with the equation below:

$$\Delta x = \frac{\partial x}{\partial slope} \Delta slope + \frac{\partial x}{\partial intercept} \Delta intercept = -0.0147A \quad (14)$$

The final calculation result of the laser threshold of this setup is: :  $x = 0.246 \pm -0.0147A$ .

The slope frequency, as we can find from the linear fit result above is :  $10.97 \pm 0.8797$ .

The relation between photon energy and photon wavelength is:

$$E = \frac{hc}{\lambda} \quad (15)$$

From the definition of quantum efficiency  $\eta$ , we have:

$$\eta = \frac{E_{lasing}}{E_{pump}} = \frac{\lambda_{pump}}{\lambda_{lasing}} = \frac{808nm}{1064nm} = 0.76 \quad (16)$$

#### 4.4.2 Pump Laser Modulation and Modes of Output Lasers

When we switched the settings of the pump laser from rectangular signal to triangular signal, we can observe two emission levels sometime. In a single-frequency laser like Nd:YAG, the output signal of the laser system could be affected by the modulation of the pump laser. When we modulated the input of pump source, the laser could quickly switch to another operation mode, at this time, both laser modes have optical power, resulting in observation of two laser modes on the oscilloscope.

### 4.5 Active Q Switching and Measurements of Critical Parameters

Our final setting of the Q Switching laser system is that the cavity length is:  $7.8 \pm 0.5mm$ . Trigger delay on the high voltage power supply is  $420\mu s$ , and the voltage of the Pockel cell was set to:  $932kV$ .

#### 4.5.1 Output pulse energy as a function of the Q-switch delay

In this part of the experiment, we measured the Q-switch delay and the maximum voltage of the spike of the output. The measurement result can be found in Table 7:

Time Delay ( $\mu$ s)	Maximum Voltage of the Spike (mV)
0	noise
20	noise
40	noise
60	noise
70	36.8 ± 4
80	120 ± 10
90	176 ± 10
100	200 ± 10
120	250 ± 10
140	220 ± 10
160	192 ± 10
180	196 ± 10
200	216 ± 10
240	148 ± 10
280	240 ± 10
320	300 ± 10
360	340 ± 10
400	376 ± 10
480	360 ± 10
530	378 ± 10
580	368 ± 10
620	216 ± 10

Table 7: Measurement Result of Output Pulse Energy and Q-switch Delay

The scatter plot of our data is shown in Figure 11:

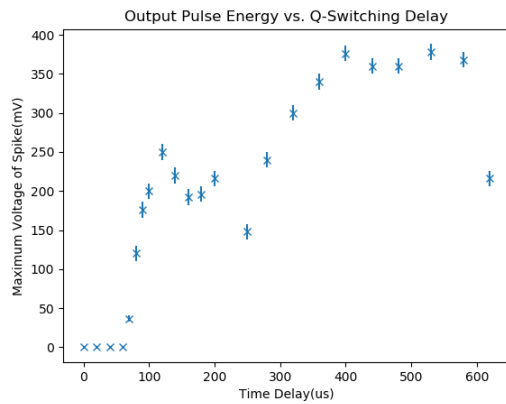


Figure 11: Scatter Plot of Out Pulse Energy and Q-switch Delay

As we can observe from the scatter plot, the maximum output peak was

observed after a delay time of  $400\mu s$ . The general trend of the statistical behavior of the two relation is that an increase in delay times lead to higher amplitude of the peaks, which eventually leads to a saturation of the amplitude of the peak. The trend we observed from these data points meet the theoretical prediction as well. As the delay time decrease, the less time will the laser system to have to reach the maximum population inversion, resulting in a lower pulse energy, thus the lower spike amplitude as observed. The saturation that occurs above  $400\mu s$  suggest that the maximum amount of population inversion of the system has been reached.

#### 4.5.2 Output Pulse Energy vs. Pump Rate

In this part of the experiment, we measured the relation between the output pulse energy and pump rate. According to Fig 20 in the lab handout, we found that the slope of the linear relation between temperature and injection current is  $-4 \frac{A}{\circ}$ . We used such relation to calculate the temperature needed to maintain constant wavelength of the laser. Our measurement data is shown in Table 8:

Temperature ( $^{\circ} C$ )	Injection Current(mA)	Peak Voltage (mV)
25	550	$364 \pm 10$
26	525	$330 \pm 10$
27	500	$285 \pm 10$
28	475	$215 \pm 10$
29	450	$130 \pm 10$
30	425	$217 \pm 10$

Table 8: Output Pulse Energy vs. Pump Rate

Excluded the last out-liner data point, we plotted the data and find the relation between pump rate and the output pulse energy, as shown in Figure 12:

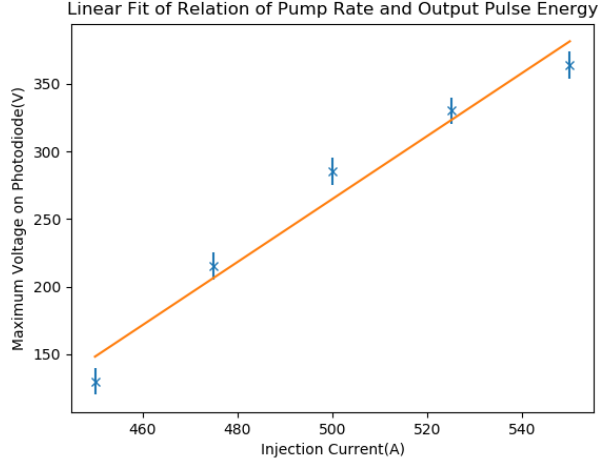


Figure 12: Linear Fit Result of Pump Rate and Output Pulse Energy

The line fitted to the data has a slope of  $2.332 \pm 0.0031$ , a intercept of  $-901.2 \pm 1.578$ , and a p-value of 0.00257. As we can see from the linear fit result, the pump rate and the pulse energy has a linear relation. The higher the pump rate, proportional to the incident power on the crystal and therefore on the injection current, the higher the pulse energy output is. This experiment result agrees with the theoretical model of an active Q-Switching by Pockel Cell. As explained in the theoretical result, the peak power is determined by Eq. (17)

$$P_p = \frac{n_p h v}{\tau_c}, \quad (17)$$

where  $n_p$  is the number of photon in the pulse. With a constant Q-switch period, when the injection current increases, the number of photons emitted during the pulse duration increases, as more electrons are pumped up when the cavity losses are high. From this, a linear trend is created between the injection current, the pump rate, the incident power on the crystal, the power emitted in the Q-switch pulse, and the voltage peak of the pulse on the oscilloscope.

It is worth delving into the details of why the voltage peak of the oscilloscope pulse corresponds to the pulse energy. The voltage on the oscilloscope is proportional to the number of photons incident on the photodiode. The pulse energy is proportional to the number of photons in the pulse, as shown in (17). Thus, the voltage on the oscilloscope will be proportional to the pulse energy. If the oscilloscope integration were shorter than the pulse, then not all of the photons in one pulse would have resulted in a voltage on the oscilloscope. Then, the voltage would not be proportional to the number of photons in the entire pulse, and thus not the pulse energy.

The minimum Q-switch delay to excite a pulse exists as a population inversion needs to build up before a pulse can be excited. The time that it takes

to build up the sufficient population inversion is inversely proportional to the pump rate and determines the minimum Q-switch delay time.

It is not possible to excite a Q-switch pulse for delays shorter than the minimal Q-switch delay because the minimal Q-Switch delay are due to the response time of the inter-grated RC circuit, which is limited by our photo-diode used in the experiment.

## 4.6 Investigation of Passive Q-Switching

In this part of the experiment, we investigated several characteristics of our passive Q-Switching system.

### 4.6.1 Frequency vs. Q-Switching Peaks

In Table 9 is the experiment result of the influence of the frequency of the laser modulation and the number of Q-Switching peaks observed on the oscilloscope.

Frequency(Hz)	Number of Peaks
427	10
399	11
375	11
349	12
324	13
300	14
290	15
275	16
250	17

Table 9: Frequency vc. Number of Q-Switching Peaks

Plotting the data, we could find a linear relation between the frequency of the laser modulation and the corresponding number of peaks, as shown in Figure 13 :

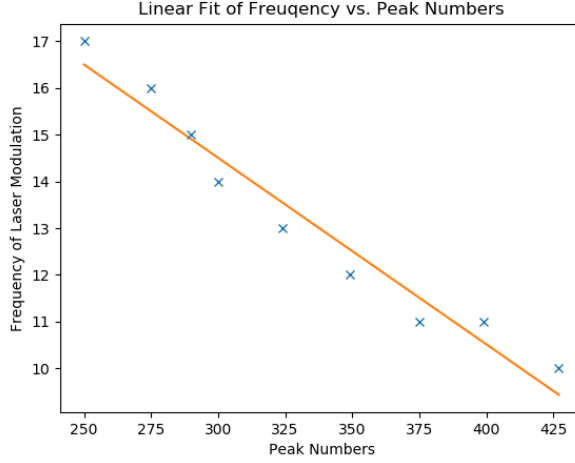


Figure 13: Frequency vs. Peak Numbers Linear Fit

As we can see, the number of peaks increases with decreasing frequency. And it follows a linear relation where the slope is  $-0.03$ , the intercept is:  $26.48$ . Because the frequency of the modulation is inverse of the period of the laser pumping source, the smaller the frequency is, the longer the period of the pumping source, the more Q-Switching can be fitted into one period.

#### 4.6.2 Pump Laser Power vs. Passive Absorber Peaks

In this part of the experiment, we changed the pump laser power from  $550\text{ mA}$  to  $425\text{ mA}$  with a step of  $25\text{ mA}$  to investigate the relation between injection current and the characteristics of the passive Q-Switching peaks. Our measurement result is shown in Table 10 , where  $I$  is the injection current,  $N$  is the number of peaks,  $T_{delay}$  is the time delay of the 1st peak of that period, and  $T_{pkTopk}$  is the distance between two peaks in the same period.

$I$ (mA)	$N$	$T_{delay}(\mu s)$	$T_{pkTopk}(\mu s)$	$V_{max}(\text{mV})$
550	16	$180 \pm 10$	$100 \pm 10$	$168 \pm 10$
525	13	$200 \pm 10$	$130 \pm 10$	$152 \pm 10$
500	11	$220 \pm 10$	$160 \pm 10$	$148 \pm 10$
475	9	$250 \pm 10$	$160 \pm 10$	$164 \pm 10$
450	8	$270 \pm 10$	$190 \pm 10$	$160 \pm 10$
425	6	$320 \pm 10$	$210 \pm 10$	$128 \pm 10$

Table 10: Injection Current vs. Peaks Characteristics

As we can observe from the table, the number of Q-Switching peaks increases as the injection current increases, meaning that more photons are emitted from

the pump laser, which makes the cycle of saturation and de-saturation of the absorber in a shorter period time, resulting in more number of peaks fitting into the time within one period of signal from the pump laser modulation . As the injection current increases, the delay time from the first peak decreases, which could be explained by the fact that more photons are emitted at the same time, thus less time will be needed for the absorber to reach the first saturation. The peak to peak distance also decreases as the injection current increase for the same reason that the increase amount of photons accelerate the process when the transmission reaches it's maximum in the absorber, resulting in the shorter peak to peak distance. The maximum voltage of the passive Q-Switching peaks shown in the data give a general trend that the maximum voltage is oscillating around a value  $160mV$ . The fluctuation of the data and uncertainty in the measurement of the maximum voltage of the peak might due to the misalignment of the setup and the pollution of the absorber.

#### 4.6.3 Absorber-YAG Rod Distance and Characters of Peaks

In Table 11 is the experiment result of the relation between distance of the absorber to the YAG rod and the measured corresponding Q-Switching peaks characters.

Distance(cm)	Number of Peaks	1st Peak Delay ( $\mu s$ )	Pk to Pk Distance ( $\mu s$ )
$1 \pm 0.1$	17	$160 \pm 10$	$130 \pm 10$
$1.5 \pm 0.1$	19	$170 \pm 10$	$130 \pm 10$
$2 \pm 0.1$	18	$160 \pm 10$	$120 \pm 10$
$2.5 \pm 0.1$	18	$180 \pm 10$	$110 \pm 10$
$3 \pm 0.1$	18	$150 \pm 10$	$110 \pm 10$
$3.5 \pm 0.1$	18	$150 \pm 10$	$80 \pm 10$

Table 11: Measurement Result of Distance of Absorber to YAG Rod and Peak Characters

As we can observe from the table, the number of peaks do not have significant change when the distance from absorber to YAG Rod increases. This is due to the fact that the process of saturation does not depend on the location of the absorber inside the cavity. The fluctuation of the data points as observed in the table might due to the misalignment of the laser system and the possible pollution of the absorber itself.

#### 4.6.4 Frequency Doubling of the Laser Wavelength

In this experiment, when we measured the relation between the pump current and the SHG output power and found the lasing threshold power. We set the injection current from 0 mA to 560 mA with a 40 mA steps. The measurement result is shown in Table 12:

Injection Current (mA)	Output Voltage(mV)
0 - 320	0
360	$1.4 \pm 1$
400	$3.8 \pm 1$
440	$10 \pm 2$
480	$18.6 \pm 1$
520	$40 \pm 1$
560	$72 \pm 2$

Table 12: Injection Current vs. SHG output power

Plotting the data using Python's matplotlib library and Scipy library, we can observe and find the linear relation between the injection current and the maximum output voltage, as shown in Figure 14:

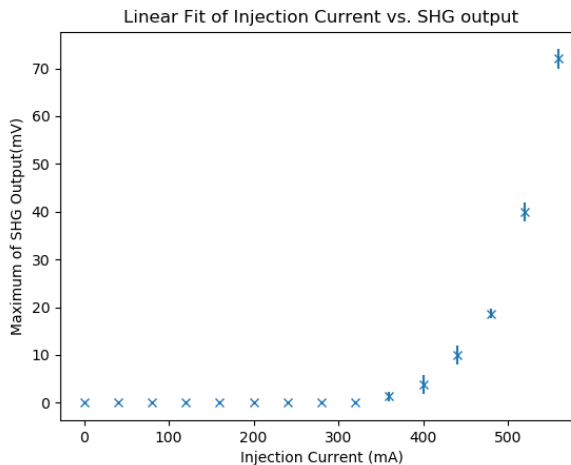


Figure 14: Injection Current vs. SHG Output

As we can see from the data taken, the laser threshold for this setup is between 320 - 360 mA. As we can observe from the plot, once the laser threshold is exceeded, the SHG output has an exponential growth with the increase of injection current. This implies that the phase-matching condition for harmonic generation is met. The reasons why this is necessarily true are discussed in the discussion.

## 5 Discussion

### 5.1 Diode Laser Characterization

#### 5.1.1 Minimum Injection Current

We got a turn-on current of 154 mA. This corresponds to typical values of diode lasers injection currents listed in literature (2).

#### 5.1.2 Pump Laser Output Power as a Function of Temperature

The result was that as temperature rises, the output power sinks linearly. This is also expected (1) (2).

The diode laser was not given much time to adjust to the temperatures higher than 30 degrees C. This introduced uncertainty in the data. In the future, in order to both have more information about this temperature range while protecting the lifetime of the diode, lower temperatures can be probed, and the data can be extrapolated into this higher-temperature zone. As the data was taken hurriedly, it was not very reliable anyway, and so rather than damage the diode laser while gathering unreliable data, extrapolation of the linear trend into this region may be sufficient for later parts, where heating up the diode laser may not be avoidable. One part where such a methodology could not be used is the determination of the transmission function of the Nd:YAG crystal, as there is no reason to assume any kind of trend. The temperature of the photodiode however is approximately linear, and so the points in this range were more of a formality than necessary to believe in the linearity of the relationship.

### 5.2 Nd: YAG Rod Characterization

#### 5.2.1 Absorption Spectrum

The Nd:YAG laser absorption peak at 808 nm agrees with the literature. Indeed, sources report an absorption peak at 808.4 nm, which is what we found (2).

### 5.3 Nd:YAG Laser Resonator

It was observed that the output power of the laser increased linearly with the power of the pump laser used. The uncertainties given in our linear fit result are very small, indicating good measurements were taken in this part of the experiment. Due to the limited amount of time given, we could not find appropriate literature to compare our result with. To further improve the accuracy of the experiment, we could take more data points by decreasing the injection current steps.

## 5.4 Active Q-Switching

As we can see from the scatter plot, in the measurement of the the relation between Q-Switch time delay and the peak amplitude of the spike, there are a few outliers of the data points that are not in good alignment with the general trend. It is possible that due to misalignment or aging of the system, errors arise from our measurement. Since all the peaks observed on the oscilloscope have different heights, we choose the highest peak as our output power, this might lead to inaccurate measurement of the data.

## 5.5 Passive Q-Switching

In our investigation of the characteristics of Q-Switching, we obtained result that meet our expectation of the behavior of the passive Q-Switching peaks. In general, the increase in frequency results in decreases of the number of peaks in one signal period. The increase in the injection current also lead to an increase in number of peaks and decrease in time delay and peak to peak distance, and the location of the absorber does not have big influence on the characteristics of the peaks as expected. However, due to the imperfection of the absorber and possible misalignment of the laser system, the fluctuation of the maximum voltage of the peaks are large. To improve the measurement result, we may improve the alignment, and replaced the aging absorber. We obtained a quantitative observation in this part of the experiment, to further investigate the characteristics of passive Q-Switching, we may collect more data points to reach a qualitative conclusion of the properties of the passive Q-Switching pulses.

# 6 Conclusion

In the first part of the experiment, we built a Nd:YAG laser system, and studied the characteristics of such system extensively. We found the optimal temperature where the Nd:YAG laser has the maximal output by measuring the absorption spectrum of the Nd:YAG laser, and explored the relation between the injection current and voltage of the output laser on the photo-diode. We also examined the Nd:YAG laser resonator by studying the relation between the pump current and laser output power.

In the second part of the experiment, we explored an active Q-Switching process using a Pockel cells and a passive Q-Switching process using a saturable absorber. We studied the passive Q-Switching process by studying the relation between output pulse energy and the Q-switch delay. We studied the characteristics of a passive Q-Switching process by studying the pulsed laser in terms of the injection current of the pump laser, the different material used for the Q-Switching processes, and the frequency of the pump laser modulation.

While most of our findings fall into our expectation and the theoretical prediction, our measurement data were slightly affected by the misalignment of the laser system and the imperfection of the components used in the experiment.

For further study, we could collect more qualitative data to investigate the effect of Q-Switching and improve the alignment of the laser system.

## 6.1 Second Harmonic Generation

The turn-on current for the SHG was high, and the resulting voltage seemed to grow exponentially afterwards. As SHG is a nonlinear phenomenon, this behavior is not a surprise. First of all, in order to make a frequency with double the energy of the initial frequency, two photons of the initial frequency are needed. This would imply that to have a steady conversion in the sense of SHG, a relatively high amount of original photons is needed. Second of all, the generated frequency being a second harmonic frequency implies that it is naturally phase-matched with the original frequency. The phase velocity of the frequency-doubled wave is twice the phase velocity of the original wave. This integer multiple in phase velocity implies a harmonic interaction between these two in space. For example, at each trough of the original 1064 nm light, the same point in the frequency doubled light's cycle would appear. This is a necessary condition for harmonic generation, and second harmonic generation in the case of reasonably temporally coherent light (as is certainly the case with laser light) is thus inherently a relatively efficient phenomenon.

## 7 References

Marcus Junghanns. *Nd:YAG Laser*. Abbe School of Photonics. March 2017.

LD Didactic. *Diode-Pumped Nd:YAG Laser*. Leybold. Accessed 3.3.2019.